We have taken two approaches in attempts to obtain the D_0 values. First, we have estimated the excited-state bond energy by a Birge–Sponer extrapolation[24] of the observed vibronic levels. In this extrapolation, a plot of the energy of a given vibrational level ($G_0(v)$) minus E_0 divided by the number of vibrational quanta (v) should yield a straight line. The dissociation energy (D_0) is then given by the square of the intercept divided by 4 times the slope.

The experimental plot is not a straight line (Figure 8). However, Birge–Sponer plots usually show negative curvature as the dissociation limit is approached, because higher terms in the vibrational energy expansion become important.[24] The positive curvature observed for $Rh_2b_4^{2+}$ at high v is probably due to the ligands; as the outer turning-point distortion at high v becomes large, the bridging groups must necessarily start to contribute to the restoring force for the vibration. We have estimated a D_0 of 42 kcal/mol from the slope derived from the vibrational levels with $v < 15$. The excited-state D_0 yields a ground-state bond energy of 18 kcal/mol.

A second estimate has been obtained from the temperature dependence of K_{eq} for the dimerization of $Rh(CNPh)_4^+$ in acetonitrile solution, resulting in the parameters $\Delta S = -15$ eu and $\Delta H = -6.3$ kcal/mol.[21] On the basis of 6 kcal/mol as the dimer ground-state D_0, the excited-state bond energy is calculated to be 30 kcal/mol. However, the value of 6 kcal/mol is likely to be an underestimate, because it neglects the differential solvation of the monomer and dimer.

If we assume that the two estimation methods define upper and lower limits, then the excited-state and ground-state Rh–Rh bond energy ranges are 36 ± 6 and 12 ± 6 kcal/mol. The values 36 and 12 kcal/mol are consistent with a well-established rule that force constants for closely related diatomic molecules are proportional to bond energies,[25] because the ratio of diatomic force constants for the $^3A_{2u}$ and $^1A_{1g}$ states is 3:1.

Acknowledgment. We thank Terry Smith for assistance with the Raman experiments. S.F.R. acknowledges a Fannie and John Hertz Fellowship. This research was supported by National Science Foundation Grant CHE84-19828.

(24) Birge, R. T.; Sponer, H. *Phys. Rev.* **1926**, *28*, 259–283.

(25) Nakamoto, K. *Infrared Spectra of Inorganic and Coordination Compounds*, 2nd ed.; Wiley-Interscience: New York, 1970; p 9.

Contribution No. 7691 from the Arthur Amos Noyes Laboratory, California Institute of Technology, Pasadena, California 91125

Vibrational and Electronic Spectra of $Ru_2(O_2CH)_4^+$

Vincent M. Miskowski,*[1a] Thomas M. Loehr,*[1b] and Harry B. Gray*[1a]

Received December 15, 1987

Vibrational (near-infrared and Raman) spectra of $Ru_2(O_2CH)_4Cl$ and $K[Ru_2(O_2CH)_4Cl_2]$ indicate values of $\nu(Ru_2) \simeq 330$ cm^{-1}, symmetric and asymmetric ν(RuCl) of 200 and 150 cm^{-1}, and ν(RuO) of ~430 (a_{1g}) and ~470 cm^{-1} (e_u). Near-infrared low-temperature electronic spectra place the $\delta \rightarrow \delta^*$ and $\pi^* \rightarrow \delta^*$ electronic transitions at ~9000 and ~7000 cm^{-1}, respectively. For both chloro complexes, and also for $[Ru_2(O_2CH)_4Br_2]^-$ (formed in KBr), three vibrations coupled to $\delta \rightarrow \delta^*$ have similar Franck–Condon factors; excited-state values are $\nu(Ru_2) \approx 275$–310 cm^{-1}, ν(RuO) ≈ 420–440 cm^{-1}, and $\nu \approx 140$–210 cm^{-1} attributable to $\delta(Ru_2O)$ or ν(Ru–halide). The vibronic intensities observed for the formate complexes are compared to those of other carboxylate derivatives, and it is concluded that strong vibrational coupling of $\nu(Ru_2)$ with other vibrational modes is present in the formates.

We recently reported[2] a comprehensive spectroscopic study of $Ru_2(O_2CR)_4X$ and $[Ru_2(O_2CR)_4X_2]^-$ (X = Cl, Br; R = methyl, ethyl, *n*-propyl). We were able to locate several metal–metal excited states of these $^4(\pi^{*2}\delta^{*1})$ ground-state compounds, including $\delta \rightarrow \delta^*$ at ~9000 cm^{-1} and the very weak spin-forbidden $\pi^* \rightarrow \delta^*$ at ~7000 cm^{-1}.

Since the available theoretical calculation[3] is for a formate complex, $[Ru_2(O_2CH)_4Cl_2]^-$, it seemed important to establish that the Ru_2(II,III) formates had electronic spectra similar to those of the other carboxylates. Photoelectron spectra[4] show that the metal–metal ionization energies of $Mo_2(O_2CH)_4$ are blue-shifted by about 1 eV from those of $Mo_2(O_2CCH_3)_4$, although their electronic transition energies are virtually the same.[5] It turns out that the transition energies also are very similar in all the Ru_2(II,III) carboxylate complexes, but the vibronic structure associated with $\delta \rightarrow \delta^*$ in the formate differs from that of the other carboxylates.

Table I. Vibrational Spectral Data (cm^{-1}) for Solid $Ru_2(O_2CH)_4Cl$ and $K[Ru_2(O_2CH)_4Cl_2]$

	$Ru_2(O_2CH)_4Cl$ (I)	$K[Ru_2(O_2CH)_4Cl_2]$ (II)
	Raman	
$\delta(Ru_2O)$	135 m	124 vw
ν_s(RuCl)	157 m	150 s
a_{1g} δ_s(RuO)	194 m	193 s
δ(RuO)	281 vw	276 vw
a_{1g} $\nu(Ru_2)$	331 vs	335 s
a_{1g} ν(RuO)	440 m	426 s
ν(RuO)	465 vw	464 vw
	IR	
δ(RuO) or δ(RuCl)		150 m
ν(RuCl)	212 s	200 s
$\nu(RuO_2)$	262 s	278 s
ν(RuO)	406 vw	405 w
	465 vs	419 w
	464 vs	464 vs
	496 s	495 s

Experimental Section

Preparations of $Ru_2(O_2CH)_4Cl$[6] and $K[Ru_2(O_2CH)_4Cl_2]$[7] followed literature procedures. Equipment and procedures used in this study were

(1) (a) California Institute of Technology. (b) Oregon Graduate Center.
(2) Miskowski, V. M.; Loehr, T. M.; Gray, H. B. *Inorg. Chem.* **1987**, *26*, 1098.
(3) Norman, J. G., Jr.; Renzoni, G. E.; Case, D. A. *J. Am. Chem. Soc.* **1979**, *101*, 5256.
(4) Cotton, F. A.; Norman, J. G., Jr.; Stults, B. R.; Webb, T. J. *J. Coord. Chem.* **1976**, *5*, 217.
(5) Norman, J. G., Jr.; Kolari, H. J.; Gray, H. B.; Trogler, W. C. *Inorg. Chem.* **1977**, *16*, 987.
(6) Mukaida, M.; Nomura, T.; Ishimori, T. *Bull. Chem. Soc. Jpn.* **1972**, *45*, 2143.
(7) Bino, A.; Cotton, F. A.; Felthouse, T. R. *Inorg. Chem.* **1979**, *18*, 259.

0020-1669/88/1327-4708$01.50/0 © 1988 American Chemical Society

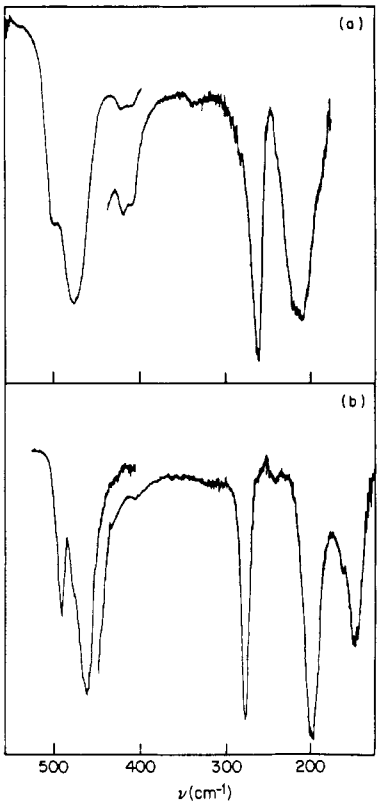

Figure 1. Far-infrared spectra of (a) $Ru_2(O_2CH)_4Cl$ and (b) $K[Ru_2(O_2CH)_4Cl_2]$ in petroleum jelly mulls at room temperature.

the same as those of our previous report.[2]

Vibrational Spectra

Vibrational spectra for the compounds $Ru_2(O_2CH)_4Cl$ (I) and $K[Ru_2(O_2CH)_4Cl_2]$ (II) are summarized in Table I. The higher frequency bands associated with formate modes are not included. We observed infrared absorption spectra typical[8,9] of this class of compound; for I, strong bands are at 1502 ($\nu_{as}(CO_2)$), 1470 ($\nu_s(CO_2)$), 1331 ($\delta(CH)$), and 771 cm^{-1} ($\delta(CO_2)$).

Far-infrared spectra are shown in Figure 1. The bands in the 400–500-cm^{-1} region are attributable to the $\nu(RuO)$ modes; they are higher frequency than those[2] of $Ru_2(O_2CCH_3)_4Cl$, 405 (e_u) and 341 cm^{-1} (a_{2u}), because of the smaller mass of formate. Assuming that the effective ligand mass is half that of the carboxylate, the formate $\nu(RuO)$ features should be higher frequency by a factor of 1.15. The most intense of these bands (475 cm^{-1} for I, 464 cm^{-1} for II) is probably e_u $\nu(RuO)$, which is expected to be intense because its normal coordinate is associated with a large dipole moment, whereas the dipole moment associated with the a_{2u} mode should be small because of ORuRu angles[7] near 90°.

We assign the strong features at ~200 cm^{-1} to $\nu(RuCl)$, as this is the frequency seen[2] for analogous acetate and butyrate complexes, where comparisons to bromide analogues established the assignment; $K[Ru_2(O_2CH)_4Cl_2]$ has been shown[7] to be structurally very similar. The bands near 270 cm^{-1} are assigned to $\delta(RuO_2)$ deformation modes;[2,9] they are, given the structural similarity, particularly the very long RuCl bonds,[7] much too high frequency to be $\nu(RuCl)$. Finally, a band of II at 150 cm^{-1} (the spectrum of I did not show any well-resolved features in this region) is attributable[2,9] to $\delta(Ru_2O)$ or $\delta(RuCl)$.

Raman spectra are shown in Figure 2. As in our previous study, red excitation was employed to minimize resonance enhancement of overtones and combinations. The spectra of I and II are very similar in terms of band position but show relative intensity variations for which we have no explanation at this time.

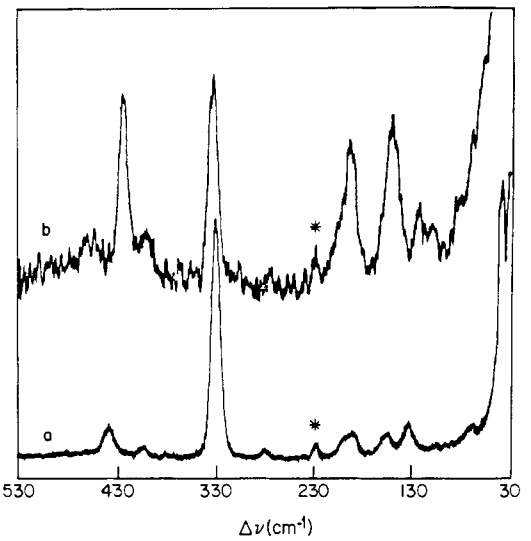

Figure 2. Raman spectra of solid samples of (a) $Ru_2(O_2CH)_4Cl$ and (b) $K[Ru_2(O_2CH)_4Cl_2]$ at room temperature with 676.4-nm (Kr^+ laser) excitation. Plasma lines are indicated with an asterisk.

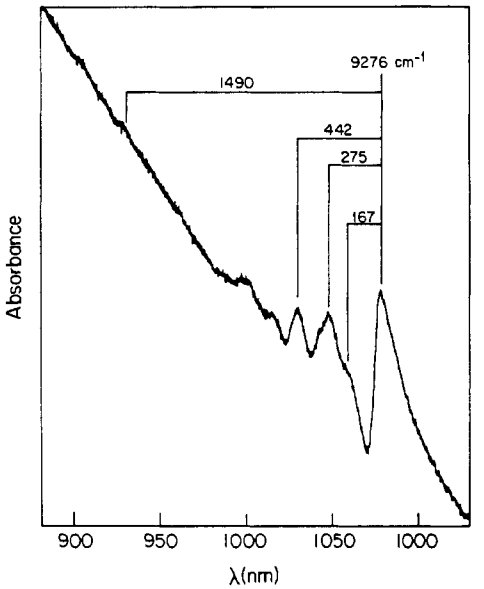

Figure 3. Electronic spectrum of $Ru_2(O_2CH)_4Cl$ in a petroleum jelly mull at 20 K.

Spectra for 647.1-nm excitation were indistinguishable from those shown.

$\nu(Ru_2)$ is readily assigned to the ~330-cm^{-1} band by reference to previous work.[2,10] The feature at ~440 cm^{-1} is assigned to the totally symmetric $\nu(RuO)$, with weak bands at ~465 and ~405 cm^{-1} probably due to non totally symmetric $\nu(RuO)$ modes, possibly $(D_{4h})b_{2g}$ and e_g, which are formally Raman-active. Preponderant intensity for the totally symmetric modes is expected from our previous work.[2] A very weak feature at ~280 cm^{-1} is attributable to $\delta(RuO_2)$, which has no totally symmetric component.

Both compounds show additional strong bands at ~195 and 150 cm^{-1}. I shows an additional feature at 135 cm^{-1}, whose intensity is possibly low-symmetry-induced. Comparison to the spectra of the other carboxylates[2] suggests assignment of the ~150 cm^{-1} band to a_{1g} $\nu(RuCl)$, and the ~195 cm^{-1} feature to a_{1g} $\delta(Ru_2O)$. This assignment is supported by a one-dimensional force-field calculation,[11] which yields force constants for the Ru_2Cl_2 unit of $k(Ru_2)$ = 2.59 mdyn/Å, $k(RuCl)$ = 0.64 mdyn/Å, and

(8) Deacon, G. B.; Phillips, R. J. *Coord. Chem. Rev.* **1980**, *33*, 227.
(9) Bratton, W. K.; Cotton, F. A.; Debeau, M. *J. Coord. Chem.* **1971**, *1*, 121.
(10) Clark, R. J. H.; Ferris, L. T. H. *Inorg. Chem.* **1981**, *20*, 2759.
(11) Herzberg, G. *Infrared and Raman Spectra of Polyatomic Molecules*; Van Nostrand: New York, 1945; pp 188–189.

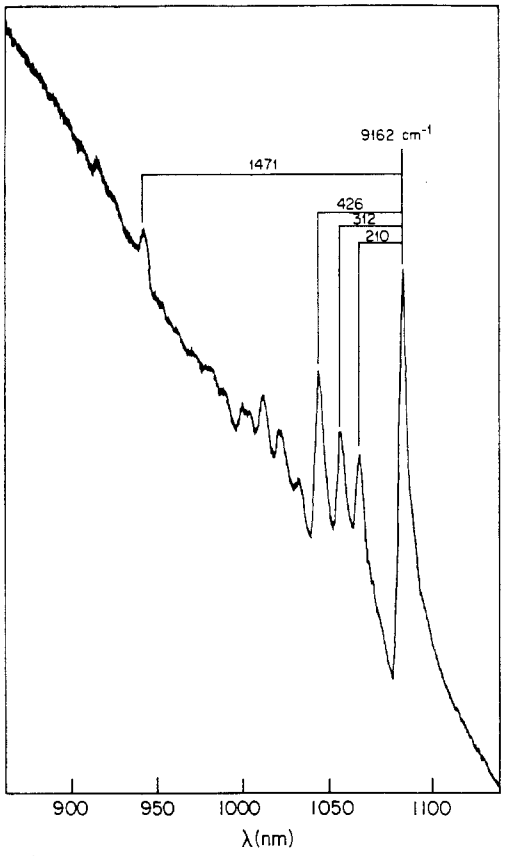

Figure 4. Electronic spectrum of $K[Ru_2(O_2CH)_4Cl_2]$ in a petroleum jelly mull at 16 K.

k(off-diagonal) = −0.012 mdyn/Å, with use of the assigned axial modes for II. These force constants are nearly identical with those previously[2] calculated for $Ru_2(O_2CCH_3)_4Cl$. On the other hand, a similar calculation, assuming the ~195-cm^{-1} band to be a_{1g} ν(RuCl), fails, yielding complex force constants.

Electronic Spectra

Visible spectra of the formates in solution[6] are nearly indistinguishable from those of the other carboxylates, implying a close electronic similarity. Low-temperature near-infrared electronic spectra of I and II (Figures 3 and 4) likewise show a $\delta \rightarrow \delta^*$ transition at nearly the same energy as seen for the other carboxylates (~9000 cm^{-1}). These spectra were obtained for petroleum jelly mulls, so individual vibronic line shapes are distorted. For both compounds it is nonetheless clear (Tables II and III) that there are three low-frequency progression-forming modes (ν_1, ν_2, ν_3). The Huang–Rhys ratios ($S = I(0 \rightarrow 1)/I(0\text{–}0)$) for all of them are fairly low (≤0.5), indicating that the excited-state distortion is small. The ν_3 values are nearly identical with the ground-state a_{1g} ν(RuO) values, while ν_2 is plausibly attributed to $\nu(Ru_2)$ that is reduced in frequency in the excited state. The higher frequency features can mostly be attributed (Tables II and III) to various combinations of ν_1, ν_2, and ν_3. However, for both compounds a new origin turns up ~1470 cm^{-1} from the electronic origin (ν_4). This is attributable to $\nu_S(CO_2)$, and its vibronic activity (yielding molecular x,y-polarized intensity) was established for the other carboxylate derivatives in previous work.[2]

Spectra were also determined in KBr pellets. The formate compounds react very efficiently with KBr. As shown in Figure 5, the KBr pellet spectrum of I shows hardly any trace of the electronic $\delta \rightarrow \delta^*$ origin seen for a mull at 9276 cm^{-1}. The strongly shifted but otherwise very analogous spectrum observed in KBr is attributed to $[Ru_2(O_2CH)_4Br_2]^-$ (III), which is formed in the matrix. The asymmetry of the origin band (9029 cm^{-1}, shoulder at 9017 cm^{-1}) and the first few vibronic features probably reflects multiple sites in the matrix. The spectrum of II in KBr is assigned mainly to III, with bands attributable to residual II as well as mixed halide ions in evidence. The assignment of the spectrum

Table II. Vibronic Features of the $\delta \rightarrow \delta^*$ Transition of $Ru_2(O_2CH)_4Cl$ in a Hydrocarbon Mull at 20 K[a]

Assignment	ν (cm⁻¹)				
o-o	9276	167	275	442	1490
ν_1	9443	154			
ν_2	9551		311	414	292
$2\nu_1$	9597				
$\nu_3, \nu_1 + \nu_2$	9718				
$2\nu_2$	9862				
$\nu_2 + \nu_3$	10010				
$2\nu_3$	10132				
ν_4	10764	141	322	447	
$\nu_4 + \nu_1$	10905				
$\nu_4 + \nu_2$	11086				
$\nu_4 + \nu_3$	11211				

[a] Average values (cm^{-1}): ν_1 = 167, ν_2 = 275, ν_3 = 442, ν_4 = 1490.

Table III. Vibronic Features of the $\delta \rightarrow \delta^*$ Transition of $KRu_2(O_2CH)_4Cl_2$ in a Hydrocarbon Mull at 16 K[a]

Assignment	ν (cm⁻¹)						
o-o	9162	210	312	426	327	427	422	1471
ν_1	9372							
ν_2	9474							
$2\nu_1, \nu_3$	9588							
$\nu_1 + \nu_2$	9699		281	432	298	289	302	
$2\nu_2, \nu_1 + \nu_3$	9799							
$\nu_2 + \nu_3, \nu_2 + 2\nu_1$	9896							
$2\nu_2 + \nu_1$	9980							
$2\nu_3, \nu_3 + 2\nu_1$	10020		386	206				
$3\nu_2$	10101							
$2\nu_2 + \nu_3, 2\nu_3 + \nu_1$	10914							
$2\nu_3 + \nu_2$	10309							
$3\nu_3$	10406							
$\nu_1 + \nu_2 + 2\nu_3$	10515							
ν_4	10633	201	320	411				
$\nu_4 + \nu_1$	10834							
$\nu_4 + \nu_2$	10953							
$\nu_4 + \nu_3$	11074							

[a] Average values (cm^{-1}): ν_1 = 210, ν_2 = 312, ν_3 = 426, ν_4 = 1471.

to III follows our previous observation[2] that the anions (e.g., II) have significantly lower energy $\delta \rightarrow \delta^*$ electronic origins than the infinite-chain $Ru_2(O_2CR)_4X$ compounds (e.g., I).

The $\delta \rightarrow \delta^*$ spectrum of III in KBr is better resolved than the mull spectra of I and II. As a result, it is evident (Table IV) that

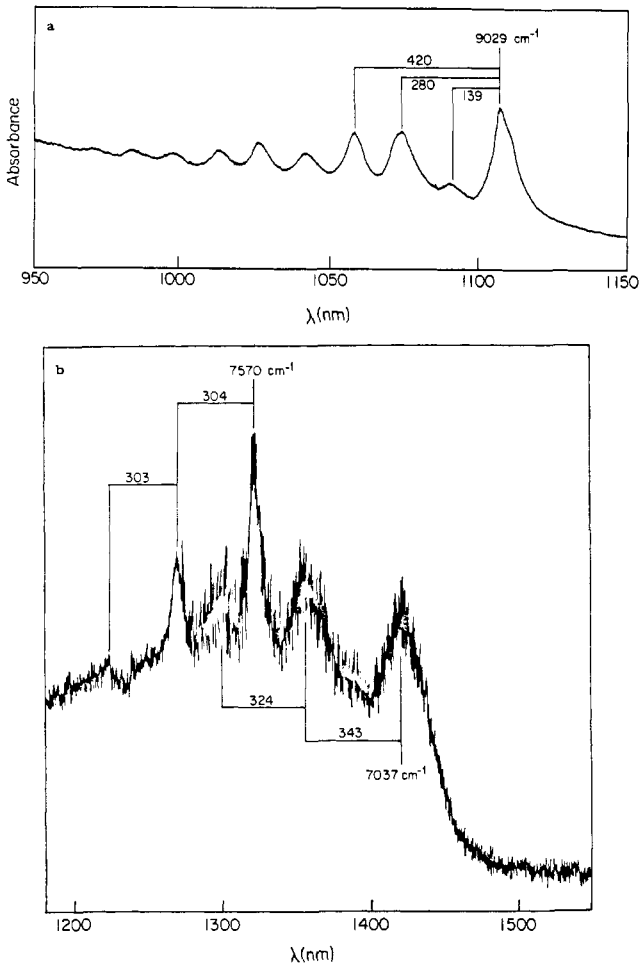

Figure 5. (a) Electronic spectrum of $Ru_2(O_2CH)_4Cl$ in a KBr pellet (2.2 mg of compound/260 mg of KBr) at 11 K. The spectrum is attributable to $[Ru_2(O_2CH)_4Br_2]^-$ formed in the matrix. (b) Expanded absorbance scale view of higher energy vibronic features of (a).

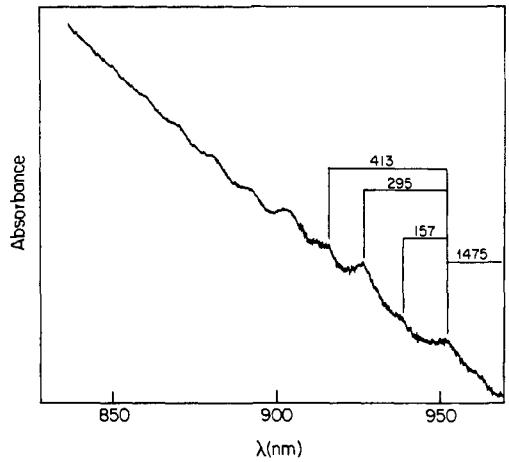

Figure 6. Electronic spectrum of $Ru_2(O_2CH)_4Cl$ in a KBr pellet (34 mg of compound/171 mg of KBr) at 16 K.

the vibronic pattern based on the electronic origin is repeated on the basis of the 1475-cm^{-1} (ν_4, the $\nu_S(CO_2)$ band) vibronic origin. The pattern is somewhat simpler than for the other compounds, because ν_1 has a lower value of S.

We also looked for the extremely weak ($\epsilon \simeq 2$) spin-forbidden $\pi^* \rightarrow \delta^*$ transition that appears[2] in the other carboxylate derivatives near 7000 cm^{-1}. It proved impossible to locate this weak band with mull samples. As shown in Figure 6, a band was observed for concentrated KBr pellets of I, with about the right extinction coefficient ($\epsilon \approx 2$). It shows a progression in $\nu(Ru_2)$ that is slightly *increased* (first quantum, 343 cm^{-1}) from the ground-state value, with larger $S(\simeq 1)$ than that seen for the $\delta \rightarrow \delta^*$ excitation; these properties are characteristic[2] of $\pi^* \rightarrow \delta^*$.

Table IV. Vibronic Features of the $\delta \rightarrow \delta^*$ Transition of a $Ru_2(O_2CH)_4Cl/KBr$ Pellet at 16 K[a]

Assignment	ν(cm⁻¹)				
0-0	9029				
		139			
ν_1	9168		280		
				420	
ν_2	9309				
		284			
$\nu_3, \nu_1 + \nu_2$	9449				
			431		
$2\nu_2$	9593			423	
$\nu_2 + \nu_3$	9740				1475
		435			
$2\nu_3, 3\nu_2$	9872				
			291		
$2\nu_2\nu_3$	10028			421	
$\nu_2 + 2\nu_3$	10163				
$3\nu_3$	10293				
		157			
ν_4	10504				
			295		
$\nu_4 + \nu_1$	10661			413	
$\nu_4 + \nu_2$	10799				
			275		
$\nu_4 + \nu_3$	10917				
				294	434
$\nu_4 + 2\nu_2$	11074				
			283		
$\nu_4 + \nu_2 + \nu_3$	11211				
				290	
$\nu_4 + 2\nu_3$	11351				414
$\nu_4 + 2\nu_2 + \nu_3$	11494				
$\nu_4 + 2\nu_3 + \nu_2$	11641				
$\nu_4 + 3\nu_3$	11765				

[a] The dominant species in the pellet is assigned to $[Ru_2(O_2CH)_4Br_2]^-$. Average values (cm^{-1}): $\nu_1 = 139$, $\nu_2 = 280$, $\nu_3 = 420$, $\nu_4 = 1475$.

A second and much sharper progression sets in at 7570 cm^{-1}. It shows a smaller progression frequency (304 cm^{-1}) and smaller S ($\simeq 0.5$). While species other than III might be present in small amounts, yielding[2] a $\pi^* \rightarrow \delta^*$ transition at slightly different energy, the progression frequency and S for the 7570-cm^{-1} band are inappropriate for a $\pi^* \rightarrow \delta^*$ assignment. The most likely assignment is to one of the several other[2] spin-forbidden transitions that could fall in this region, one possibility being $\delta^* \rightarrow \pi^*$. However, in the absence of single-crystal data, impurities such as $Ru_2(O_2CH)_4$ or $Ru_2(O_2CH)_4Br_2$ cannot be excluded as the origin of this very weak electronic absorption.

Vibronic Assignments for the $\delta \rightarrow \delta^*$ Transition

It is clear from the similarity in electronic transition energies for the formates and the previously studied carboxylates that there are no significant differences in metal–metal bonding among these compounds. However, both in the vibrational spectra and in the vibronic structure of the $\delta \rightarrow \delta^*$ transition, we do see significant differences.

For butyrate and propionate complexes, we have found that $\nu(Ru_2)$ dominates the vibronic structure of $\delta \rightarrow \delta^*$. Weak vibronic origins were seen for a_{1g} $\nu(RuO)$ and $\delta(CO_2)$, and e_g $\nu(CO_2)$, $\nu(RuO)$, and $\delta(Ru_2O)$ transitions were also observed. For acetate complexes, it was found that a_{1g} $\nu(Ru_2)$ (ground-state $\nu \approx 330$ cm^{-1}) and a_{1g} $\nu(RuO)$ (ground-state $\nu \approx 370$ cm^{-1}) had similar values of S for the $\delta \rightarrow \delta^*$ transition, and a large ground-state vibrational coupling of these two modes, prompted by a frequency difference much smaller than for the other carboxylates, was proposed to be the explanation for the considerable Franck–Condon activity of $\nu(RuO)$.

The formate results indicate a more complicated situation. Despite a large frequency separation of a_{1g} $\nu(Ru_2)$ and $\nu(RuO)$, they have similarly large S values for the $\delta \rightarrow \delta^*$ transition. Moreover, yet a third vibration, ν_1 of Tables II–IV, has a similar S value.

In view of the constancy of the ground-state geometry and the $\delta \rightarrow \delta^*$ electronic transition energy among the various ruthenium carboxylates, it seems highly unlikely that $\delta \rightarrow \delta^*$ excited-state distortions are changing among them. Thus, a vibrational coupling, with a predominant distortion remaining along the metal–metal coordinate, is likely responsible for the formate results.

The bridged $M_2(O_2CR)_4$ structure necessarily imposes a coupling among the totally symmetric $\nu(M_2)$, $\nu(MO)$, and $\delta(OM_2)$ modes. We think that the key to understanding the formate results is that the bridging ligand is exceptionally light among those of the compounds examined. Accordingly, the low amplitude changes in MO bond distance to be associated with a "pure" M_2 distortion are closer to those associated with $\nu(MO)$ than is true for the heavier carboxylates (larger effective masses, hence larger amplitudes for $\nu(MO)$) for a given frequency. Thus, vibrational coupling is expected, so long as the frequency difference between the modes is not large, and this remains true for the formate compounds.

We have thus far avoided assignment of ν_1 in the $\delta \rightarrow \delta^*$ transitions of the formates. The most likely assignment, following the above analysis, is to $\delta(OM_2)$, uniquely strongly active for the formate bridging ligand. However, the frequency of ν_1 varies strongly among compounds I, II, and III, suggesting the possibility that the mode might be $\nu(RuX)$. Additionally, we do not possess single-crystal data for the formates, so it remains possible that ν_1 might be a non totally symmetric mode,[2] and the assignment is therefore doubtful.

We emphasize that vibronic intensity profiles for nominally pure metal–metal excitations such as $\delta \rightarrow \delta^*$ may, without any change in electronic structure of ground and excited states, be strongly perturbed by vibrational coupling effects. We think that the effects seen here are somewhat peculiar to the $M_2(O_2CR)_4$ structure, with its tight coupling of internal motions, and the interpretation of the vibronic structure of electronic transitions of unbridged binuclear compounds is probably simpler. In a bridged case, a great deal of caution is, however, desirable in the interpretation of vibronic structure.

We wish to comment on a probable additional example of such effects. Martin and co-workers[12] have reported that $Mo_2(O_2CH)_4$ in its various polymorphic crystalline forms exhibits, in addition to progressions in $\nu(Mo_2)$ ($\sim$350 cm^{-1}), two strong vibronic origins $\sim$380–390 and $\sim$770–780 cm^{-1} above the $^1(\delta \rightarrow \delta^*)$ electronic origin. It was noted that these frequencies were considerably higher than for "analogous" features[13] of the $^1(\delta \rightarrow \delta^*)$ transition of $Mo_2(O_2CCH_3)_4$. It is likely that the 380–390-cm^{-1} origin is the excited-state $\nu(MoO)$, whose frequency reasonably is much larger[14] than for the acetate (assigned[13] at 275 cm^{-1}), and that the 770–780-cm^{-1} origin is simply $2\nu(MoO)$. Both of these assignments are consistent with what we have observed for $\delta \rightarrow \delta^*$ of the ruthenium formate complexes but were not considered by Martin et al.,[12] presumably because they appeared to be inconsistent with the interpretation of the $^1(\delta \rightarrow \delta^*)$ system of the acetate.

Acknowledgment. This research was supported by National Science Foundation Grant CHE84-19828.

(12) (a) Robbins, G. A.; Martin, D. S. *Inorg. Chem.* **1984**, *23*, 2086. (b) Robbins, G. A. Ph.D. Dissertation, Iowa State University, Ames, IA, 1982.
(13) Martin, D. S.; Newman, R. A.; Fanwick, P. E. *Inorg. Chem.* **1979**, *18*, 2511.
(14) The ground-state frequency has not been assigned. Raman bands for $Mo_2(O_2CH)_4$ have been reported[4] at 420, 406 ($\nu(Mo_2)$), 393, 371, and 350 cm^{-1}.

Contribution from the Department of Chemistry,
University of Pittsburgh, Pittsburgh, Pennsylvania 15260

Spin Trapping of Superoxyl and Hydroxyl Radical Complexes of Ruthenium(II) and -(IV) Polyaminopolycarboxylates

Songsheng Zhang and Rex E. Shepherd*

Received January 28, 1988

$Na[Ru^{II}(hedta)(H_2O)]\cdot 4H_2O$ has been oxidized in solution by $Na_2S_2O_8$ to form a Ru^{IV} complex, isolated as $Ru_2O(hedta)_2\cdot(15.4 \pm 0.4)H_2O$. Cyclic voltammetry and Na^+ analysis supports a bridging Ru–O–Ru structure; analogous results were obtained for $Ru^{II}(edta)^{2-}$. Ru^{III} complexes formed in the H_2O_2 or O_2 oxidation of $Ru^{II}(edta)^{2-}$, $Ru^{II}(hedta)(H_2O)^-$, and $Ru^{II}_2(tha)(H_2O)_2^{2-}$ also undergo water replacement by H_2O_2. The bound $(L)Ru^{III}(O_2^{2-})$ species (L = $edta^{4-}$, $hedta^{3-}$, $ttha^{6-}$) exhibit substantial $(L)Ru^{II}(O_2^-)$ character, forming spin adducts with DMPO. The $LRu^{II}(O_2^-)$DMPO adducts exhibit a seven-line ESR pattern of intensities nearly 1:2:2:2:2:2:1 with couplings $A_N \simeq 8.0$ G, $A_{H_\beta} \simeq A_{H_\gamma} \simeq 5.0 \pm 0.5$ G for L = $ttha^{6-}$, $edta^{4-}$ and $A_N = 10.0$ G, $A_{H_\beta} \simeq A_{H_\gamma} \simeq 5.0$ G for $hedta^{3-}$. The couplings are independent of D_2O in the solvent. No DMPO radical adducts are observed with $Ru^{II}L$, $Ru^{III}L$, or $Ru^{IV}L$ complexes alone. Oxidation of $Ru^{II}L$ or $Ru^{III}L$ complexes with $(CH_3)_3COOH$ generates a different radical species, trappable by DMPO. The spin adduct has the character of Ru^{III}–O atom or $Ru^{IV}(OH^\bullet)$, giving rise to a triplet of triplets pattern. The spectral intensity decreases with increasing percentage of D_2O in the solvent. This shows an exchangeable proton is present that couples in the spin adduct. Couplings are $A_N = 7.5$ G, A_H (2 equivalent H couplings) = 4.2 G (L = $edta^{4-}$), 4.0 G ($hedta^{3-}$). The spin adduct is therefore assigned as the $LRu^{IV}(OH)$DMPO species. The Ru^{III}–O atom species epoxidize olefin bonds while the $Ru^{II}(O_2^-)$ species add to olefins, giving nonradical products. Thus, the O atom channel mimics aspects of monooxygenase systems and the superoxo channel mimics aspects of dioxygenase systems.

Introduction

The reduction of O_2 and H_2O_2 by transition-metal reductants is a long-standing chemical problem. It impinges on the autoxidations of a diverse array of inorganic and organic substrates, as well as metabolic reactions in biological cells. Coordinated oxygen radicals are the proposed intermediates in oxygen activation by dioxygenases and monooxygenases.[1,2] The hydroxylations and epoxidations carried out by these enzymes are attributed to $Fe^{III}(O_2^-)$ (superoxo) and $Fe^{II}(O_2^-)$ (superoxo) $\leftrightarrow$ $Fe^{III}(O_2^{2-})$ (peroxo) species. The superoxo complexes are capable of radical addition to double bonds[1] while the peroxo species can participate in O atom transfer reactions. The reactive entity in the peroxo case may be more properly assigned to the ferryl Fe^{III}–O atom species if cleavage of the O–O bond, liberating H_2O, precedes atom

(1) Ochiai, E.-I. *Bioinorganic Chemistry, An Introduction*; Allyn and Bacon: Boston, 1977; Chapters 7 and 10.
(2) Hamilton, G. A. In *Molecular Mechanisms of Oxygen Activation*; Hayaishi, O., Ed.; Academic Press: New York, 1974.

0020-1669/88/1327-4712$01.50/0 © 1988 American Chemical Society